



A selection method of variable speed centrifugal pumps for maximum hydraulic efficiency

Yahia M. Fouda¹

Received: 1 February 2023 / Accepted: 9 September 2023 / Published online: 3 October 2023
© The Author(s) 2023

Abstract

Variable speed pumps (VSPs) are more energy efficient compared to other flow control methods such as throttling control valves. However, their selection process is not straightforward because the pump characteristics should be optimised against the load profile of the flow system for maximum hydraulic efficiency. This paper presents a VSPs selection method based on generic mathematical models of centrifugal pumps efficiency, characteristics and similitude, which enables the extension of this method to other types of turbomachines. This selection method results in a nonlinear algebraic equation that is solved numerically to obtain a reference flow rate that maximises the pumping system hydraulic efficiency. This reference flow rate is subsequently used to obtain the pump characteristic curves at all operating pump speeds. The results show that this method is fast, accurate and reliable. Because the developed method uses generic pump models rather than specific models from manufacturers' databases, it enables the integration of VSP selection process in early engineering design phases of pumping systems.

Keywords Variable speed pumps · Centrifugal pumps · Pump selection · Flow systems · Energy efficiency · Hydraulic efficiency

List of symbols

Roman letters

a	Ratio of reference and operating heads
b	Ratio of reference and operating flow rates
c, d, e	Derivation parameters (symbols)
E_H	Hydraulic energy
F	Flow calculation function
g	Acceleration of gravity
m	Number of system states
H	Head
Q	Flow rate
q	Ratio of actual flow rate to that at BEP
W	Work

Greek letters

α, β, γ	Pump coefficients
Ψ	Work percentage
Δt	Operating time
η	Efficiency
ρ	Fluid density
θ, ϵ	Modified pump parameters

Subscripts

0	Best operating point
i	System state
m	Maximum
R	Reference rotational speed of the pump
T	Total

Superscripts

n	Iteration number
-----	------------------

Technical Editor: Daniel Onofre de Almeida Cruz.

✉ Yahia M. Fouda
Yahia_Fouda@mans.edu.eg

¹ Department of Mechanical Power Engineering, Faculty of Engineering, Mansoura University, Mansoura 35516, Egypt

1 Introduction

Centrifugal pumps are dynamic work-absorbing turbomachines used to increase the pressure of liquid flows in order to meet specific demands of flow systems. Centrifugal pumps transfer energy to liquids using a rotating impeller

that increases the momentum of the fluid. Centrifugal pumps are designed so that the cross-sectional area of flow passages inside the pump increases as the fluid flows from the suction side to the discharge side. Thus, the increase in the fluid momentum is converted to increase in its pressure. Centrifugal pumps are essential components in fluid flow systems; they are widely used in different industrial sectors such as power generation, oil and gas, water distribution networks, process industries and heating, ventilation and air conditioning (HVAC). The average energy consumption of these industrial pumping systems is around 90% of the total life cycle costs of the pumps [1]. Thus, increasing the efficiency of centrifugal pumps reduces the operating costs of fluid pumping system, especially for over-sized low-efficiency pumping systems, which constitute significant percentage of industrial pumping system [2]. Moreover, increasing the efficiency of centrifugal pumps contributes towards meeting national and international targets in reducing carbon footprint [1].

Increasing the efficiency of a pumping system is achieved by examining its energy conversion processes in order to reduce the energy losses in each of these processes. A typical pumping system consists of a prime mover used to supply the required work to rotate the pump impeller. This prime mover could be an electric motor, internal combustion engine or turbine. Increasing the efficiency of energy conversion in the prime mover is not related directly to the pump itself. However, both pump and prime mover should be selected so that their mechanical characteristics—rotational speed and torque—match, which enable them to operate close to their maximum efficiency simultaneously [3]. Moreover, the mechanical coupling between the prime mover and the pump should be selected so that the shaft transmission losses are minimised. Other types of energy losses in a pumping system include the hydraulic losses of the pump, which results from the conversion efficiency of the shaft work to hydraulic energy; and the hydraulic efficiency of the fluid flow system itself, which results from the hydraulic losses in fluid flow conduits such as pipes, valves and fittings.

It is not uncommon for pumping systems to operate at variable loads in order to meet variable flow demands. For example, it has been reported that HVAC pumping systems operate at maximum loads for only 6% of their total operating time [4]. Thus, increasing the pumping system efficiency in partial loading enhances its overall operating efficiency significantly. In order to achieve partial loading of a fluid pumping system, the flow rate could be reduced by either using a throttling control valve, or reducing the rotational speed of the pump using a variable speed drive (VSD) [3, 5], among other mechanisms. Using throttling control valves increases the hydraulic energy losses significantly because the pressure losses increase as the fluid flows across a

partially open control valve. Moreover, throttling forces the pump to operate at lower efficiency compared to its best efficiency point (BEP), which is a specific operating point defined by unique values of pressure difference and flow rate for each pump model. On the other hand, achieving the partial loading requirements of a pumping system by reducing the pump rotational speed using VSD eliminates these two losses mechanisms. By reducing the pump rotational speed, the power delivered to the pumping system is not in excess. Thus, there is no need to dissipate the energy in the system. Moreover, one could ensure that the pump operates close to its BEP at each rotational speed corresponding to each partial loading requirement, which also reduces the mechanical loads on the pump components due to the reduction in its rotational speed [6, 7]. Thus, VSD is a natural fit in pumping applications when there is a strong variation in the system load profile with time.

When the load profile of the flow system is nearly constant with time, the pump selection process is rather simple—a fixed speed pump model is selected so that its BEP almost coincides with the system operating point. For systems which operate at variable loads, however, selecting a VSP is not as straightforward in all cases because the overall performance of the pump at different partial loads should be optimised in order to achieve maximum efficiency [4, 8]. For systems with low or zero static head, i.e. dynamic head systems, the selection process of VSP is similar to that of fixed speed pumps. This is because the pump characteristics can be chosen so that its best efficiency line (BEL) nearly coincides with the system curve. For static head systems, on the other hand, it is difficult, or nearly impossible, to choose a VSP whose BEL coincides with the system curve [9]. However, some general qualitative recommendations exist in such selection process [9]. Another point to consider in VSP selection is the performance metric—the method used to calculate the overall efficiency of variable speed pumping systems. The overall efficiency of such systems is not a simple averaging of individual efficiencies at each rotational speed. It depends, however, on the efficiencies of the operating points, their time of operation and their power. In order to accurately consider all these factors, a performance metric, referred to as true weighted efficiency (TWE), which is equivalent to the overall system efficiency, has been developed to assist in selecting VSPs [4, 8].

The aim of this paper is to develop a VSP selection method based on generic centrifugal pump models—efficiency, characteristics and similitude—rather than using commercial pump models from manufacturers' databases, which enables to include VSPs in the conceptual design or planning of fluid networks [6]. The derivation of this method maximises the overall hydraulic efficiency, or the TWE, of the pumping system. This derivation results in a single non-linear algebraic equation which is solved numerically in

order to obtain the pump characteristic curve. Subsequently, all the other relevant information, including speed reduction ratios, are obtained.

2 Problem formulation

Consider a fluid pumping system that operates at m different states. Each state of this system is defined by an integer index $i \in \{1, m\}$ and characterised by a given hydraulic operating point—head, H_i , and discharge, Q_i —and operating time, Δt_i . In order to meet the flow requirements of this system, a variable speed pump (VSP), which operates at an efficiency η_i corresponding to the system state i , is used. The total work absorbed by this VSP, W_T , is the summation of the work at each state, W_i , which is expressed as

$$W_T = \sum_{i=1}^m W_i = \sum_{i=1}^m E_{H,i}/\eta_i = \sum_{i=1}^m \rho g H_i Q_i \Delta t_i / \eta_i, \tag{1}$$

where $E_{H,i}$ is the hydraulic energy delivered by the pump, ρ is the fluid density, and g is the acceleration of gravity. The total work of the pump can also be expressed in terms of the total hydraulic energy, $E_{H,T}$, and the overall hydraulic efficiency, η_T , as

$$W_T = E_{H,T} / \eta_T = \left(\sum_{i=1}^m \rho g H_i Q_i \Delta t_i \right) / \eta_T, \tag{2}$$

Eqs. (1) and (2) are equal,

$$\left(\sum_{i=1}^m H_i Q_i \Delta t_i \right) / \eta_T = \sum_{i=1}^m H_i Q_i \Delta t_i / \eta_i. \tag{3}$$

Thus, the reciprocal of the overall efficiency is

$$1/\eta_T = \sum_{i=1}^m \Psi_i / \eta_i, \tag{4}$$

where Ψ_i is the work percentage defined as the ratio of the hydraulic energy delivered at each state i with respect to the total hydraulic energy,

$$\Psi_i = H_i Q_i \Delta t_i / \left(\sum_{i=1}^m H_i Q_i \Delta t_i \right). \tag{5}$$

The aim of this paper is to select a variable speed pump (VSP) that maximises the overall hydraulic efficiency η_T of this fluid pumping system, which is identical to the TWE [4, 8]. VSP selection means determining its characteristics (HQ curve) at each state i . In the following analysis, it is assumed that the pump suction pressure is well above vapour pressure so that the pump inlet pressure is within its net positive

suction head (NPSH), which means that cavitation does not take place.

2.1 Pump hydraulic efficiency

The hydraulic efficiency of a centrifugal pump, η_i , operating at a specific rotational speed can be expressed as a quadratic equation of the flow rate, Q_i , as [1, 10–12]

$$\eta_i = \alpha_i + \beta_i Q_i + \gamma_i Q_i^2. \tag{6}$$

The efficiency is zero at zero flow rate [1, 3, 10–12]

$$\eta_i(Q_i = 0) = 0, \tag{7}$$

which results in

$$\alpha_i = 0. \tag{8}$$

Furthermore, the efficiency is zero at maximum flow rate, $Q_{i,m}$ because this flow rate corresponds to zero head,

$$\eta_i(Q_i = Q_{i,m}) = 0, \tag{9}$$

which results in

$$\beta_i = -Q_{i,m} \gamma_i. \tag{10}$$

Substituting Eqs. (9) and (10) into Eq. (6) results in

$$\eta_i = -\gamma_i Q_{i,m} Q_i + \gamma_i Q_i^2. \tag{11}$$

By definition, the efficiency is maximum at the optimal flow rate, $Q_{i,0}$. Thus, the first derivative of the efficiency η_i with respect to the flow rate vanishes at $Q_{i,0}$, which is expressed mathematically as

$$\frac{d\eta_i}{dQ_i}(Q_i = Q_{i,0}) = -\gamma_i Q_{i,m} + 2\gamma_i Q_{i,0} = 0, \tag{12}$$

where the parameters α_i , β_i and γ_i are constants for a given rotational speed.

Solving Eq. (12) results in the following relation between the maximum flow rate and the flow rate at BEP, $Q_{i,0}$,

$$Q_{i,m} = 2Q_{i,0}. \tag{13}$$

Substituting Eq. (13) into Eq. (11) results in

$$\eta_i = \gamma_i Q_i (Q_i - 2Q_{i,0}). \tag{14}$$

Since the efficiency is maximum at BEP, a maximum efficiency coefficient, $\eta_{i,m}$, can be defined by setting $Q_i = Q_{i,0}$ in Eq. (14) as

$$\eta_{i,m} = -\gamma_i Q_{i,0}^2. \tag{15}$$

Thus, for a given rotational speed, it is possible to express the parameter γ_i in terms of the maximum efficiency $\eta_{i,m}$ as

$$\gamma_i = -\frac{\eta_{i,m}}{Q_{i,0}^2}. \quad (16)$$

Substituting Eq. (16) into Eq. (14) results in the pump efficiency equation as

$$\eta_i = -\frac{\eta_{i,m}Q_i}{Q_{i,0}^2}(Q_i - 2Q_{i,0}). \quad (17)$$

Thus, for a given value of $\eta_{i,m}$, the hydraulic efficiency at a given rotational speed, η_i , is a function of both the known flow rate, Q_i , and the flow rate at BEP, $Q_{i,0}$.

Equation (17) can be written as

$$\eta_i = -\eta_{i,m}\frac{Q_i}{Q_{i,0}}\left(\frac{Q_i}{Q_{i,0}} - 2\right). \quad (18)$$

Define the ratio of the actual flow rate to that at BEP as

$$q_i = Q_i/Q_{i,0}. \quad (19)$$

Thus, the pump hydraulic efficiency can be written as

$$\eta_i = -\eta_{i,m}q_i(q_i - 2). \quad (20)$$

2.2 Pump characteristics

In this paper, the pump head, H_i , is expressed as a parabolic relation in the flow rate [1, 12] as

$$H_i = \theta_i - \epsilon_i Q_i^2, \quad (21)$$

where θ_i and ϵ_i are the pump parameters, which should have positive values so that the standard shape of the pump characteristic curve is obtained. At BEP, both the pump head and flow rate are at their optimum values, $H_{i,0}$ and $Q_{i,0}$. Thus, the HQ relation at BEP based on Eq. (21) is

$$H_{i,0} = \theta_i - \epsilon_i Q_{i,0}^2, \quad (22)$$

which allows to express θ_i in terms of ϵ_i and $H_{i,0}$ as

$$\theta_i = H_{i,0} + \epsilon_i Q_{i,0}^2. \quad (23)$$

Substituting Eq. (23) into Eq. (21) results in

$$H_i = H_{i,0} + \epsilon_i(Q_{i,0}^2 - Q_i^2). \quad (24)$$

Furthermore, the pump head vanishes at the maximum flow rate, $Q_{i,m}$, which is twice the optimum flow rate, $Q_{i,0}$, as given by Eq. (13). Substituting Eq. (13) into Eq. (24) at $H_i = 0$ results in the following expression for ϵ_i

$$\epsilon_i = H_{i,0}/(3Q_{i,0}^2). \quad (25)$$

Substituting Eq. (25) into Eq. (24) results in the pump characteristic equation being

$$H_i = H_{i,0}\left(1 + (Q_{i,0}^2 - Q_i^2)/(3Q_{i,0}^2)\right). \quad (26)$$

Rewrite Eq. (26) in terms of q_i as given by Eq. (19) as

$$H_i = H_{i,0}(4 - q_i^2)/3. \quad (27)$$

The final form of the pump efficiency and characteristics, given by Eqs. (20) and (27), respectively, are expressed in terms of the maximum efficiency, optimum flow and optimum head. These equations will be used to derive a maximum efficiency equation for a VSP operating at different loads for known time intervals.

2.3 Pump similitude

In order to relate the pump characteristics and efficiency at different rotational speeds, affinity laws must be applied to VSP. There are two types of affinity laws: generic [13], which are based on pump dimensional analysis; and empirical [14], which are based on performance data of a specific pump model. In this paper, generic affinity laws are used in order to derive a generic model for selecting VSP. However, the following analysis approach could be extended to other affinity laws of specific pump models.

Generic affinity laws for VSP state that at two different rotational speeds, the head and flow rate ratios at BEP are related as

$$(H_{R,0}/H_{i,0}) = (Q_{R,0}/Q_{i,0})^2 = q_{i,0}^2, \quad (28)$$

where $H_{R,0}$ and $Q_{R,0}$ are the BEP head and flow rate at a reference rotational speed of the pump, respectively.

Equation (28) implies that the characteristics (HQ curves) of the pump are parallel at different rotational speeds. This is because the ratio $H_{i,0}/Q_{i,0}^2$, which is constant, is the slope of HQ curves, $3\epsilon_i$, as shown by Eq. (26). This does not necessarily mean that the maximum efficiencies at all rotational speeds, $\eta_{i,m}$, are equal. It means, however, that the normalised efficiency, $\eta_i/\eta_{i,m}$, as given by Eq. (20), does not vary with the pump rotational speed. This was confirmed for specific pump models [3], whereby all $\eta_i/\eta_{i,m}$ curves almost collapse for different rotational speeds.

It is possible to write q_i , which is defined by Eq. (19), as

$$q_i = \frac{Q_i}{Q_{i,0}} = \left(\frac{Q_i}{Q_R}\right)\left(\frac{Q_R}{Q_{R,0}}\right)\left(\frac{Q_{R,0}}{Q_{i,0}}\right), \quad (29)$$

where Q_R is the actual flow rate of a known reference operating condition. Thus, it is possible to set Q_R equal to any of

the known flow rates. In this paper, Q_R is equal to the flow rate at the pump rated (maximum operating) speed.

Now, define other flow rate ratios as

$$\left(\frac{Q_i}{Q_R}\right) = a_i, \quad \left(\frac{Q_R}{Q_{R,0}}\right) = q_R, \quad \left(\frac{Q_{R,0}}{Q_{i,0}}\right) = q_{i,0}. \tag{30}$$

Thus, Eq. (29) can be written as

$$q_i = a_i q_R q_{i,0}. \tag{31}$$

Since a_i can be computed using the given flow rates at operating conditions (Q_i), and q_i is a function of both q_R and $q_{i,0}$, the overall efficiency, η_T , defined by Eq. (4), becomes a function of a single independent variable, q_R , if $q_{i,0}$ could be represented as a function of q_R . Rewrite Eq. (27) as

$$H_{i,0} = 3H_i / (4 - q_i^2). \tag{32}$$

Similarly, the reference head at BEP, $H_{R,0}$, is expressed as

$$H_{R,0} = 3H_R / (4 - q_R^2). \tag{33}$$

Divide Eq. (33) by Eq. (32) and substitute into Eq. (28) results in

$$\left(\frac{H_{R,0}}{H_{i,0}}\right) = \left(\frac{H_R}{H_i}\right) \left(\frac{4 - q_i^2}{4 - q_R^2}\right) = q_{i,0}^2. \tag{34}$$

Similar to the definition of a_i which is given by Eq. (30), the ratio of the reference head, H_R , to the operating head, H_i , is defined as

$$b_i = H_R / H_i. \tag{35}$$

Substituting Eq. (35) into Eq. (34) gives

$$q_{i,0}^2 = b_i (4 - q_i^2) / (4 - q_R^2). \tag{36}$$

By definition, the values of the head and flow rate ought to be positive, which means that the values of both q_R and q_i should be between 0 and 2. Thus, the square root of Eq. (36) is its positive root as

$$q_{i,0} = \sqrt{b_i} \left(\frac{4 - q_i^2}{4 - q_R^2}\right)^{0.5}. \tag{37}$$

Substituting Eq. (37) into Eq. (31) gives

$$q_i = q_R \left(a_i \sqrt{b_i}\right) \left(\frac{4 - q_i^2}{4 - q_R^2}\right)^{0.5}. \tag{38}$$

The variables in Eq. (38) are separated using some mathematical manipulation, resulting in q_i being a function of q_R as

$$q_i = \frac{d_i q_R}{\sqrt{1 + e_i q_R^2}}, \tag{39}$$

where

$$c_i = a_i^2 b_i, \tag{40}$$

$$e_i = (c_i - 1) / 4, \tag{41}$$

$$d_i = \sqrt{c_i}. \tag{42}$$

2.4 Maximum overall hydraulic efficiency

In order to obtain q_R which maximises the overall efficiency, η_T , or minimises its reciprocal, $1/\eta_T$, the first derivative of Eq. (4) is set equal to zero, while noting that Ψ_i is constant, which results in the following expression:

$$\frac{d(1/\eta_T)}{dq_R} = \sum_{i=1}^m \Psi_i \frac{d(1/\eta_i)}{dq_R} = 0. \tag{43}$$

The right-hand side of Eq. (43) is obtained by using the chain rule as

$$\frac{d(1/\eta_i)}{dq_R} = \frac{\partial(1/\eta_i)}{\partial q_i} \frac{dq_i}{dq_R}. \tag{44}$$

In order to obtain $\partial(1/\eta_i)/\partial q_i$ as a function of $\partial\eta_i/\partial q_i$, the following equation is used

$$(1/\eta_i)\eta_i = 1, \tag{45}$$

whose first derivative is

$$\frac{\partial}{\partial q_i} ((1/\eta_i)\eta_i) = 0. \tag{46}$$

Expanding Eq. (46) results in

$$(1/\eta_i) \frac{\partial\eta_i}{\partial q_i} + \eta_i \frac{\partial(1/\eta_i)}{\partial q_i} = 0, \tag{47}$$

which can be written as

$$\frac{\partial(1/\eta_i)}{\partial q_i} = -(1/\eta_i^2) \frac{\partial\eta_i}{\partial q_i}. \tag{48}$$

In order to obtain $\partial\eta_i/\partial q_i$, it is assumed that $\eta_{i,m}$ is not a function of q_i , i.e. $\eta_{i,m}$ is constant for all rotational speeds. It was shown that this assumption is valid for up to 30% reduction of the pump nominal speed [1]. Empirical correlations expressing $\eta_{i,m}$ as a function of the pump rotational speed have been reported in the literature [15, 16]. Those correlations were accurate in predicting the variable speed

efficiency for small pumps [15, 17]. However, they were not as accurate as assuming constant $\eta_{i,m}$ for all rotational speeds up to 30% speed reduction in large pumps [15, 17]. Thus, one cannot reach a universal conclusion on such issue. In this paper, it is assumed that $\eta_{i,m}$ is constant for all rotational speeds because such assumption results in a generic model, which is the aim of this paper. However, other empirical correlations for $\eta_{i,m}$ could be employed using the following approach with additional mathematical manipulation.

Assuming that $\eta_{i,m}$ is not a function of q_i , the first derivative of Eq. (20) is

$$\frac{\partial \eta_i}{\partial q_i} = 2\eta_{i,m}(1 - q_i). \tag{49}$$

Thus, the first term on the right-hand side of Eq. (44) is

$$\frac{\partial(1/\eta_i)}{\partial q_i} = \frac{2(q_i - 1)}{\eta_{i,m}q_i^2(q_i - 2)^2}. \tag{50}$$

The second term on the right-hand side of Eq. (44) is the first derivative of Eq. (39), as

$$\frac{dq_i}{dq_R} = \frac{d_i}{\sqrt{1 + e_i q_R^2}} \left(1 - \frac{e_i q_R^2}{1 + e_i q_R^2} \right), \tag{51}$$

which, after some mathematical manipulation, is written as

$$\frac{dq_i}{dq_R} = d_i(1 + e_i q_R^2)^{-3/2}. \tag{52}$$

In order to obtain the final form of Eq. (44), substitute Eqs. (50) and (52) into Eq. (44) as

$$\frac{d(1/\eta_i)}{dq_R} = 2 \left(\frac{d_i}{\eta_{i,m}} \right) \left(\frac{q_i - 1}{q_i^2(q_i - 2)^2} \right) (1 + e_i q_R^2)^{-3/2}. \tag{53}$$

Finally, substitute Eq. (53) into Eq. (43) as

$$\frac{d(1/\eta_T)}{dq_R} = \sum_{i=1}^m 2 \left(\frac{d_i \Psi_i}{\eta_{i,m}} \right) \frac{(q_i - 1)}{(q_i(q_i - 2))^2} (1 + e_i q_R^2)^{-3/2} = 0, \tag{54}$$

which can be written, using Eq. (39), as

$$F(q_R) = \frac{d(1/\eta_T)}{dq_R} = \sum_{i=1}^m 2 \left(\frac{\Psi_i}{\eta_{i,m}} \right) \left(\frac{q_i - 1}{(q_i - 2)^2} \right) \left(\frac{(1 + e_i q_R^2)^{-1/2}}{d_i q_R^2} \right) = 0 \tag{55}$$

In order to obtain q_R which maximises the overall efficiency, η_T , Eq. (55) is solved numerically, with q_i being a function

of q_R as shown by Eq. (39). Subsequently, Eq. (19) is used to obtain all other flow rates at BEP, $Q_{i,0}$. Then, the heads at BEP, $H_{i,0}$ are obtained using the HQ curves given by Eq. (27), which means the VSP has been selected. The efficiency of each state, η_i , is obtained by Eq. (20). Subsequently, the overall hydraulic efficiency of the pumping system, η_T , is obtained by using Eq. (4). Since it has been assumed that the maximum hydraulic efficiency at a given pump speed, $\eta_{i,m}$, is constant, which is expressed mathematically as

$$\eta_{i,m} = \eta_m; \tag{56}$$

therefore, the results for both state and overall efficiency, η_i and η_T , will be normalised by η_m in the rest of this paper.

2.5 Numerical solution method

Equation (55) is solved numerically using Newton–Raphson iterative method. The new value of q_R^{n+1} at the $n + 1$ iteration is calculated as

$$q_R^{n+1} = q_R^n - \frac{F(q_R^n)}{F'(q_R^n)} \tag{57}$$

The first derivative of Eq. (55), $F'(q_R^n)$, is obtained numerically using the finite difference method. Because the range of q_i is between 0 and 2, the solution search is restricted within this range. When $q_i = 1$, the contribution of this specific q_i in Eq. (55) is zero, i.e. $F_i(q_R) = 0$, which means that the operating point coincides with the BEP at this rotational speed. Note that $F_i(q_R) > 0$ when $q_i > 0$ and vice versa. Thus, the function $F(q_R)$ can be zero in Eq. (55) if all values of q_i are unity or if they are distributed around unity so that their contributions to $F(q_R)$ are equally distributed around zero.

When the operating point corresponds to the reference operating point, $q_i = q_R$, Eqs. (30), (35), (40) and (41) show that $a_i = b_i = c_i = d_i = 1$. Furthermore, Eq. (42) shows that $e_i = 0$. Thus, the following relation holds:

$$F_i(q_R) = 2 \left(\frac{\Psi_i}{\eta_{i,m}} \right) \left(\frac{q_R - 1}{q_R^2(q_R - 2)^2} \right). \tag{58}$$

It is clear from Eqs. (55) and (58) that the two critical values of q_R are 0 and 2. To study the equation behaviour at these two points, substitute these two values in Eq. (39):

- If $q_R = 0$, then $q_i = 0$ and $F(q_R) = -\infty$.
- If $q_R = 2$, then, using Eqs. (41) and (42), $q_i = 2$ and $F(q_R) = \infty$.

Since the range of the function varies between $-\infty$ and ∞ , Eq. (55) should have at least one root—at least one q_R that maximises the overall efficiency, η_T , between 0 and 2. During the numerical solution of Eq. (55), it was noticed that

Table 1 Case studies [18, 19]

System	S1	S2	S3	S4	S5
Number of states (m)	5	4	7	6	6
$\min(Q_i)/\max(Q_i)$ (%)	72.5	35	59	50	50
$\min(H_i)/\max(H_i)$ (%)	83	96	91	88	33

Table 2 S1 system states [18]

State index (i)	1	2	3	4	5
State index (i)	1	2	3	4	5
Flow rate (m^3/s)	0.145	0.16	0.176	0.19	0.2
Head (m)	29	30	32	34	35
Time (h)	108	151	173	104	212

using different initial guess, q_R^0 , leads to the same solution, confirming that there is one value of q_R within the valid range which maximises the overall efficiency, η_T .

3 Results and discussion

In this section, the developed VSP selection method is tested using five realistic cases studies [18, 19] which are shown in Table 1. The inputs of the developed selection method are the system states: flow rate Q_i , head H_i and time of operation Δt_i . Note that the speed reduction for cases S2-S5 is higher than the recommended 30% [3, 15, 17]. Thus, the overall hydraulic efficiency is expected to be lower than that predicted for these case studies. Nevertheless, this does not affect the validity of the findings because the aim of this comparison is to show the effects of work percentage and static head variation on the selected VSPs.

3.1 VSP selection for maximum overall hydraulic efficiency

In order to show the results of the developed VSP selection method, a system with high static head [18], referred to as S1, is used in this section. The system states are shown in Table 2. The minimum flow rate is 72.5% of the maximum flow rate, whereas the minimum head, corresponding to the minimum flow rate, is around 83% of the maximum head.

Figure 1 shows the characteristics of the selected VSP, its BEL, and its operating points—flow rate and head—for the system S1. It is clear that the pump is selected so that the system curve starts at the right of the pump BEL for the maximum operating point which corresponds to the highest pump speed. As the pump speed is reduced, the

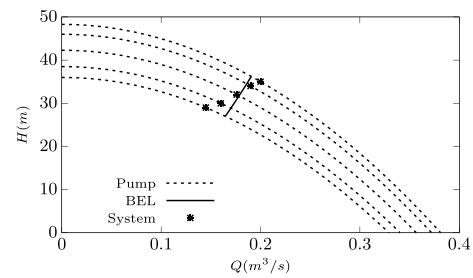


Fig. 1 Pump characteristics curve, operating points and BEL for system S1

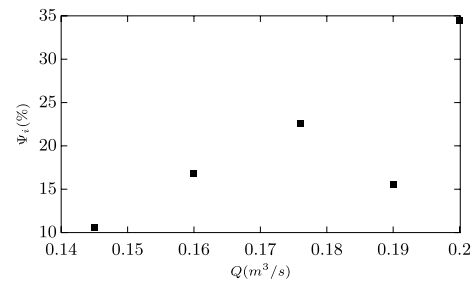


Fig. 2 Work percentage for different operating points for system S1

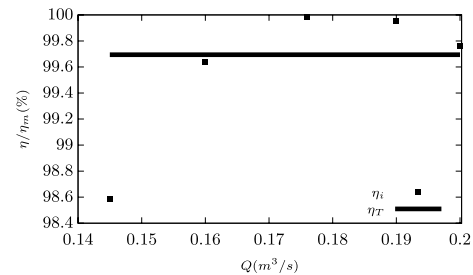


Fig. 3 Normalised efficiency of different operating points and overall efficiency for system S1

system curve crosses the BEL ending at the left of the BEL for the minimum operating point which corresponds to the lowest pump speed. This behaviour is the recommended selection approach for systems with high static head [9]. It is also clear that the operating point of the lowest pump speed is located far from the BEL compared to those of the higher speed. This is due to the work percentage distribution of the system, which is shown in Fig. 2. The work percentage of the point with the lowest flow rate (state 1 in Table 2) is around 10%. Thus, the pump is selected so that its characteristics are biased against that point, as shown in the definition of TWE in Eqs. (4) and (5). Thus, the overall normalised efficiency of the pumping system is closer to the efficiencies of states 2–5 as shown in Fig. 3.

Table 3 S2 system states [18]

State index (<i>i</i>)	1	2	3	4
Flow rate (m^3/s)	0.04	0.063	0.09	0.113
Head (m)	46	47	47.5	48
Time (h)	561	756	56	43

3.2 Effect of work percentage

This section presents a comparison between the selected VSPs for two systems with high static head, S2 and S3 [18]. The operating states of S2 and S3 are shown in Table 3 and Table 4, respectively. For S2, the minimum flow rate is 35% of the maximum flow rate, whereas the minimum head is around 96% of the maximum head. For S3, on the other hand, the minimum flow rate is 59% of the maximum flow rate, whereas the minimum head is around 91% of the maximum head.

Figure 4 shows the characteristics curves of the selected VSP, its BEL, and the system operating points for S2 (a) and S3 (b). Similar to Fig. 1, the pump is selected so that the maximum operating point, corresponding to the highest pump speed, starts, for both S2 and S3, at the right of BEL, then goes to the left as the pump speed is reduced, crossing the BEL in between. For S2, the operating point of the highest pump speed is located far from the BEL compared to that of the lowest speed. This is due to the work percentage distribution of the system, which is shown in Fig. 5. The operating point of S2 whose flow rate is $0.063 m^3/s$, i.e. state 2 in Table 3, has the highest share of the total work—around 60%. This is because its operating time is very high compared to other states, although it is not the point of the highest power. On the contrary, the operating point of the lowest pump speed for S3 is located far from the BEL compared to that of the highest speed. This is because the last four points account for around 80% of the total work, as shown in Fig. 5. It is thus shown in Fig. 6 that the VSP is selected, for each system, so that it has the highest normalised efficiency at the states of the highest work percentage. Again, this confirms that this selection method is biased towards the operating states which require higher work percentage, as shown in the definition of TWE in Eqs. (4) and (5).

Table 4 S3 system states [18]

State index (<i>i</i>)	1	2	3	4	5	6	7
Flow rate (m^3/s)	0.145	0.16	0.18	0.207	0.225	0.235	0.245
Head (m)	49	50	51	52	52.5	53.5	54
Time (h)	108	65	108	151	173	104	212

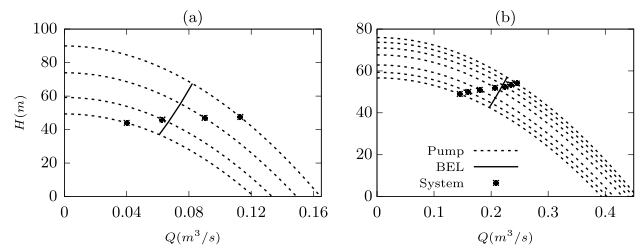


Fig. 4 Pump characteristics curve, operating points and BEL a S2, b S3

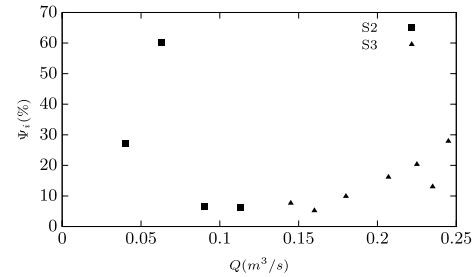


Fig. 5 Work percentage for different operating points, S2 and S3

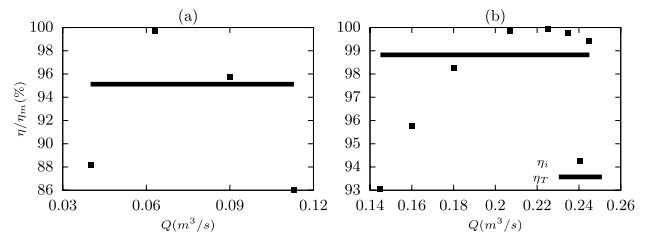


Fig. 6 Normalised efficiency of different operating points and overall efficiency. a S2, b S3

3.3 Effect of static and dynamic head

Here, a comparison between the selected VSPs of two systems, S4 and S5 [19], whose operating states are shown in Table 5, is presented. In the work of Salmasi et al. [19], the system head is defined by a quadratic equation which is a function of its operating flow rate. The intercept of this equation, A , is the value of the system static head. In this paper, the system S4 is defined using the same equation, whereas the system S5 is defined by setting $A = 0$ so that the system includes dynamic head only. This is done in order to investigate the effect of static head variation on the selected VSPs.

Table 5 S4 ($A = 45.296$) and S5 ($A = 0$) system states [19]

State index (i)	1	2	3	4	5	6
Flow rate (m^3/s)	0.04	0.052	0.047	0.039	0.03	0.026
Head (m)	$2519.1Q^2 + 64.064Q + A$					
Time (h)	15.432	19.208	16.581	15.513	16.363	16.714

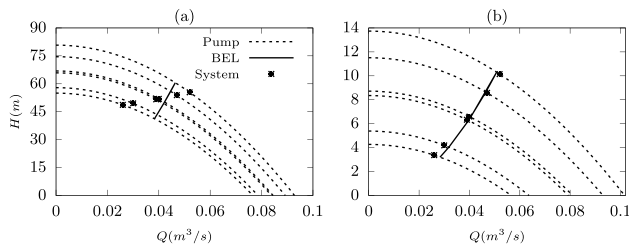


Fig. 7 Pump characteristics curve, operating points and BEL. **a** S4, **b** S5

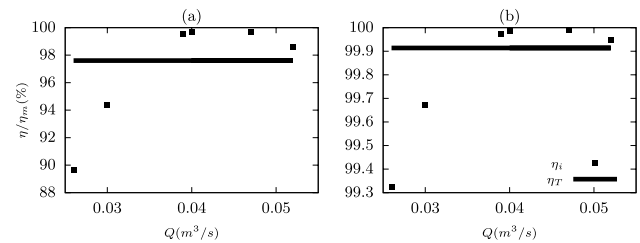


Fig. 9 Normalised efficiency of different operating points and overall efficiency. **(a)** S4, **(b)** S5

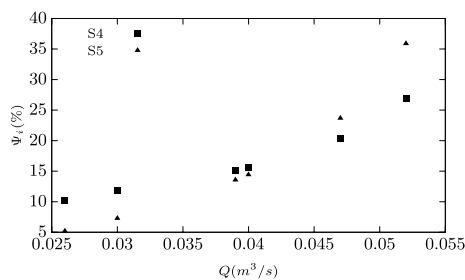


Fig. 8 Work percentage for different operating points, S4 and S5

For S4, the minimum flow rate is 50% of the maximum flow rate, whereas the minimum head is around 88% of the maximum head. For S5, on the other hand, the minimum flow rate is 50% of the maximum flow rate, whereas the minimum head is around 33% of the maximum head.

Figure 7 shows the characteristics curves of the selected VSP, its BEL, and the system operating points for S4 and S5. Because S4 is dominated by static head, its behaviour is similar to S1, S2 and S3. For the system S5, which includes dynamic head only, its BEL almost passes through all the operating points because the intercept of the HQ equation is zero. Thus, the parabolic relation of the selected pump shown in Eq. (18) can almost be fitted with the quadratic relation of the system equation shown in Table 5 with $A = 0$.

Figure 8 shows the work percentage of both systems S4 and S5. For both systems, it is clear that the distributions of the work percentage have similar trends, though the distribution is quantitatively different between the two systems S4 and S5. This is because the system equation of S5 is the same as S4 but without its vertical axis intercept, i.e. its static head. The normalised efficiency distribution is thus qualitatively similar as shown in Fig. 9. The efficiency

of S5 is indeed higher than that of S4 because its operating points almost coincide with the BEL of the selected pump.

4 Conclusions

This paper presented a VSPs selection method based on generic mathematical models of centrifugal pumps. The equations describing the pump efficiency, characteristics and similitude were combined resulting in, after appropriate mathematical manipulation, a single nonlinear algebraic equation that maximises the pumping system overall hydraulic efficiency. This equation is a function of a reference flow rate and is solved numerically using Newton–Raphson method. This reference flow rate is subsequently used to obtain the pump characteristic curves at all operating pump speeds. The overall hydraulic efficiency equation used in this paper takes into account the efficiencies of the operating points, their time of operation and their power. The selection method presented in this paper could be extended to other models of centrifugal pumps using different equations describing the pump efficiency, characteristics and similitude as well as other types of turbomachines.

Five case studies of real pumping systems obtained from the literature [18, 19] were investigated in order to assess the developed method. It is shown that:

1. The developed method selects a VSP whose characteristics are biased towards the system states with the highest work percentage, which is significant for systems with high static head.

- The behaviour of the selected VSPs for systems with high static head is similar to the qualitative recommendations in the literature [9].
- It is possible to select VSPs for systems with dynamic head only whose BEL almost coincides with the system curve, on the contrary to systems with high static head.

The results show that this method is fast because it requires the numerical solution of a single equation; accurate because it results in VSPs with high efficiency; and reliable because it is capable of operating with different flow curves and head profiles. Since this method uses generic pump models rather than specific models from manufacturers' databases, it enables the integration of VSP selection in early engineering design phases of pumping systems.

Author's contributions Not applicable.

Funding Open access funding provided by The Science, Technology & Innovation Funding Authority (STDF) in cooperation with The Egyptian Knowledge Bank (EKB). The author declares that no funds, grants or other support were received during the preparation of this manuscript.

Availability of data and material The manuscript includes all the necessary data to replicate this study.

Declarations

Conflict of interest The author has no relevant financial or non-financial interests to disclose.

Ethical approval Not applicable.

Consent to participate Not applicable.

Consent to publish Not applicable.

Open Access This article is licensed under a Creative Commons Attribution 4.0 International License, which permits use, sharing, adaptation, distribution and reproduction in any medium or format, as long as you give appropriate credit to the original author(s) and the source, provide a link to the Creative Commons licence, and indicate if changes were made. The images or other third party material in this article are included in the article's Creative Commons licence, unless indicated otherwise in a credit line to the material. If material is not included in the article's Creative Commons licence and your intended use is not permitted by statutory regulation or exceeds the permitted use, you will need to obtain permission directly from the copyright holder. To view a copy of this licence, visit <http://creativecommons.org/licenses/by/4.0/>.

References

- Briceño-León CX, Iglesias-Rey PL, Martínez-Solano FJ, Morameliá D, Fuertes-Miquel VS (2021) Use of fixed and variable speed pumps in water distribution networks with different control strategies. *Water* 13(4):479. <https://doi.org/10.3390/w13040479>
- Waide P, Brunner CU (2011) Energy-efficiency policy opportunities for electric motor-driven systems. Working paper, IEA
- Stoffel B (2015) Assessing the energy efficiency of pumps and pump units. Elsevier, Boston. <https://doi.org/10.1016/B978-0-08-100597-2.00001-X>
- Dahl T (2021) Optimizing pump and compressor selection for energy efficiency using true-weighted efficiency (TWE), pp. 741–759. Springer, Cham. https://doi.org/10.1007/978-3-030-69799-0_52
- Kaya D, Yagmur EA, Yigit KS, Kilic FC, Eren AS, Celik C (2008) Energy efficiency in pumps. *Energy Convers Manage* 49(6):1662–1673. <https://doi.org/10.1016/j.enconman.2007.11.010>
- Wu W, Simpson AR, Maier HR, Marchi A (2012) Incorporation of variable-speed pumping in multiobjective genetic algorithm optimization of the design of water transmission systems. *J Water Resources Plan Manage* 138(5):543–552. [https://doi.org/10.1061/\(ASCE\)WR.1943-5452.0000195](https://doi.org/10.1061/(ASCE)WR.1943-5452.0000195)
- Hovstadius G (2001) Life-cycle strategy for pumps improves cost structure. *World Pumps* 2001(413):30–32. [https://doi.org/10.1016/S0262-1762\(01\)80061-4](https://doi.org/10.1016/S0262-1762(01)80061-4)
- Dahl T (2018) The theory and application of true weighted efficiency—a new metric to evaluate pump energy efficiency considering multiple operating conditions. In: Proceedings of the 47th turbomachinery and 34th pump symposia
- Europump and hydraulic institute: variable speed pumping. Elsevier Science, Amsterdam (2005). <https://doi.org/10.1016/B978-185617449-7/50001-X>
- Karaca M, Aydin M (2013) Efficient driving at variable speeds. *World Pumps* 2013(4):38–41. [https://doi.org/10.1016/S0262-1762\(13\)70125-1](https://doi.org/10.1016/S0262-1762(13)70125-1)
- Muszyński P (2010) Impeller pumps: relating η and n . *World Pumps* 2010(7):25–29. [https://doi.org/10.1016/S0262-1762\(10\)70198-X](https://doi.org/10.1016/S0262-1762(10)70198-X)
- Alandi PP, Pérez PC, Álvarez JFO, Hidalgo MÁM, Martín-Benito JMT (2005) Pumping selection and regulation for water-distribution networks. *J Irrigat Drain Eng* 131(3):273–281. [https://doi.org/10.1061/\(ASCE\)0733-9437\(2005\)131:3\(273\)](https://doi.org/10.1061/(ASCE)0733-9437(2005)131:3(273))
- Arun Shankar VK, Umashankar S, Paramasivam S, Hanigovszki N (2016) A comprehensive review on energy efficiency enhancement initiatives in centrifugal pumping system. *Appl Energy* 181:495–513. <https://doi.org/10.1016/j.apenergy.2016.08.070>
- Pérez-Sánchez M, López-Jiménez PA, Ramos HM (2018) Modified affinity laws in hydraulic machines towards the best efficiency line. *Water Resources Manage* 32:829–844. <https://doi.org/10.1007/s11269-017-1841-0>
- Coelho B, Andrade-Campos AG (2016) A new approach for the prediction of speed-adjusted pump efficiency curves. *J Hydraul Res* 54(5):586–593. <https://doi.org/10.1080/00221686.2016.1175521>
- Sárbu I, Borza I (1998) Energetic optimization of water pumping in distribution systems. *Period Polytech Mech Eng* 42(2):141–152
- Simpson AR, Marchi A (2013) Evaluating the approximation of the affinity laws and improving the efficiency estimate for variable speed pumps. *J Hydraul Eng* 139(12):1314–1317. [https://doi.org/10.1061/\(ASCE\)HY.1943-7900.0000776](https://doi.org/10.1061/(ASCE)HY.1943-7900.0000776)
- Lamaddalena N, Khila S (2012) Energy saving with variable speed pumps in on-demand irrigation systems. *Irrigat Sci* 30:157–166. <https://doi.org/10.1007/s00271-011-0271-7>
- Salmasi F, Abraham J, Salmasi A (2022) Evaluation of variable speed pumps in pressurized water distribution systems. *Appl Water Sci* 12:51. <https://doi.org/10.1007/s13201-022-01577-8>

Publisher's Note Springer Nature remains neutral with regard to jurisdictional claims in published maps and institutional affiliations.